9066–9076 *Nucleic Acids Research, 2021, Vol. 49, No. 16* *Published online 7 August 2021*
https://doi.org/10.1093/nar/gkab664

The lane-switch mechanism for nucleosome repositioning by DNA translocase

Fritz Nagae[1], Giovanni B. Brandani[1], Shoji Takada[1] and Tsuyoshi Terakawa[1,2,*]

[1]Department of Biophysics, Graduate School of Science, Kyoto University, Kyoto, Japan and [2]PRESTO, Japan Science and Technology Agency (JST), Kawaguchi, Japan

Received April 20, 2021; Revised July 18, 2021; Editorial Decision July 21, 2021; Accepted July 26, 2021

ABSTRACT

Translocases such as DNA/RNA polymerases, replicative helicases, and exonucleases are involved in eukaryotic DNA transcription, replication, and repair. Since eukaryotic genomic DNA wraps around histone octamers and forms nucleosomes, translocases inevitably encounter nucleosomes. A previous study has shown that a nucleosome repositions downstream when a translocase collides with the nucleosome. However, the molecular mechanism of the downstream repositioning remains unclear. In this study, we identified the lane-switch mechanism for downstream repositioning with molecular dynamics simulations and validated it with restriction enzyme digestion assays and deep sequencing assays. In this mechanism, after a translocase unwraps nucleosomal DNA up to the site proximal to the dyad, the remaining wrapped DNA switches its binding lane to that vacated by the unwrapping, and the downstream DNA rewraps, completing downstream repositioning. This mechanism may have broad implications for transcription through nucleosomes, histone recycling, and nucleosome remodeling.

INTRODUCTION

Nucleosomes are building blocks of eukaryotic chromosomes and contribute to packaging of genomic DNA into small nuclei. A nucleosome occludes ∼147 bp of DNA wrapping around a histone octamer from the proteins involved in DNA transactions (DNA replication, transcription and repair) (1,2). DNA translocases (e.g. DNA/RNA polymerases, replicative helicases and exonucleases) unidirectionally move along genomic DNA using nucleotide triphosphate hydrolysis energy (3). Translocases frequently move longer distances than the typical lengths of linker DNA (20–50 bp) between adjacent nucleosomes without dissociation (4). For example, human RNA polymerase II (Pol II) transcribes DNA by translocating on the ∼2.5 Mbp dystrophin gene (5). Therefore, translocases inevitably collide with nucleosomes (2,6,7).

In a cellular environment, translocases and histone chaperones cooperatively reposition or dismantle nucleosomes through their specific interaction with the histone octamers (8). The interaction between a translocase with a histone octamer plays important roles in the repositioning. For example, previous studies proposed that Pol II repositions nucleosomes by specifically interacting with the histone octamer (by the so-called Pol II-type mechanism) (9–16). In this mechanism, a translocase passes through a nucleosome without changing the histone octamer position by electrostatically interacting with the octamer.

However, to unravel the roles of the interaction between a translocase with a histone octamer during repositioning, a translocase having no specific interaction with the octamer has served as a simple model system. In the previous studies, Studitsky and Felsenfeld *et al*. performed *in vitro* restriction enzyme digestion assays and showed that a nucleosome repositions upstream when SP6 or T7 RNA polymerase (RNAP) partially unwraps nucleosomal DNA (9,17–20). Since RNA polymerase III (Pol III) shows the same behavior, this mechanism is called the Pol III-type mechanism (21). Notably, in these assays, nucleosomes were reconstituted at the end of DNA, precluding downstream repositioning.

On the other hand, Greene *et al*. performed single-molecule imaging experiments and showed that a nucleosome repositions downstream when a bacterial exonuclease, RecBCD, collides with it (6). In this imaging, nucleosomes were reconstituted at random positions on the λ phage genomic DNA, thus not precluding downstream repositioning. However, sub-kbps spatial resolution of the single-molecule imaging prevented them from proposing molecular mechanisms of the downstream repositioning. While Luger *et al*. proposed the pushing mechanism in which one base-pair unwrapping is coupled to one base-pair downstream repositioning, the molecular detail of this mechanism have not been explored (22).

In this study, we performed coarse-grained molecular dynamics (MD) simulations, proposed the lane-switch mechanism for downstream repositioning, and validated this

*To whom correspondence should be addressed. Tel: +81 75 753 4220; Fax: +81 75 753 4222; Email: terakawa@biophys.kyoto-u.ac.jp

mechanism by restriction enzyme digestion assays and micrococcal nuclease digestion with deep sequencing (MNase-seq) assays. In this mechanism, after a translocase unwraps nucleosomal DNA up to the site proximal to the dyad, the remaining wrapped DNA switches its binding region (lane) to that vacated by the unwrapping, and subsequently the downstream DNA rewraps, completing downstream repositioning. This mechanism may significantly improve our understanding of the molecular basis of transcription through nucleosomes, histone recycling, and nucleosome remodeling in a more complex cellular environment.

MATERIALS AND METHODS

Coarse-grained MD simulations

We performed coarse-grained MD simulations in which a translocase was fixed in space and nucleosome reconstituted 275 bp DNA which was threaded through the translocase was pulled so that the nucleosome collides with the translocase (Figure 1A). In this setup, the translocase relatively moves toward the nucleosome. We used the AICG2 + model (23) for a histone octamer, and the 3SPN.2C model (24) for DNA. In the AICG2 + model, each amino acid is represented by one bead placed on the C_α atom of each residue. In the 3SPN.2C model, each nucleotide is represented by three beads placed at the centers of mass of phosphate, sugar, and base groups. The nucleosome structure with Widom 601 strong nucleosome-positioning DNA sequence was modeled based on the crystal structures (PDB ID: 1KX5 (25) and 3LZ0 (26)) (Figure 1B), and 32 and 96 bp DNA strands were added upstream and downstream of the nucleosome, respectively, to make sure that there is no nucleosome positioning sequence except the Widom 601 sequence (Supplementary Table S1). The same potential energy functions as previous studies were used to stabilize the nucleosome structure (27).

In the simulations, we modeled a translocase as a torus. The potential energy function of the excluded volume term of the torus (Supplementary Figure S1) is

$$V_{torus} = \sum_{i}^{N} V_{torus,i} \ ,$$

where N is the total number of particles and

$$V_{torus,i} = \begin{cases} 0 & (d_i > r^u) \\ 4\varepsilon\left[\left(\frac{\sigma}{d_i}\right)^{12} - \left(\frac{\sigma}{r^u}\right)^{12}\right] & (r^l < d_i \le r^u) \\ 4\varepsilon\left[\left(\frac{\sigma}{r^l}\right)^{12}\left(1 + 12\left(\frac{r^l - d_i}{r^l}\right)\right) - \left(\frac{\sigma}{r^u}\right)^{12}\right] & (d_i \le r^l) \end{cases} .$$

$r^u = 3.0\sigma$ and $r^l = 0.8\sigma$ define the upper and lower boundaries of the potential energy function (the second line) smoothly connecting the functions for inside (the third line) and outside (the first line) of the torus. The distance between the surface of the torus and the i-th particle in cylindrical coordinates is

$$d_i = \| \mathbf{r}_i\,(x,\ r, \theta) - \mathbf{r}_i\,(0,\ d_{M_r},\ \theta)\ \| \ - d_{m_r},$$

where d_{M_r} and d_{m_r} are the major and minor radii of the torus, respectively. $\mathbf{r}_i(x,\ r,\ \theta)$ is the position of the protein and DNA particles. In all simulations, we set the potential

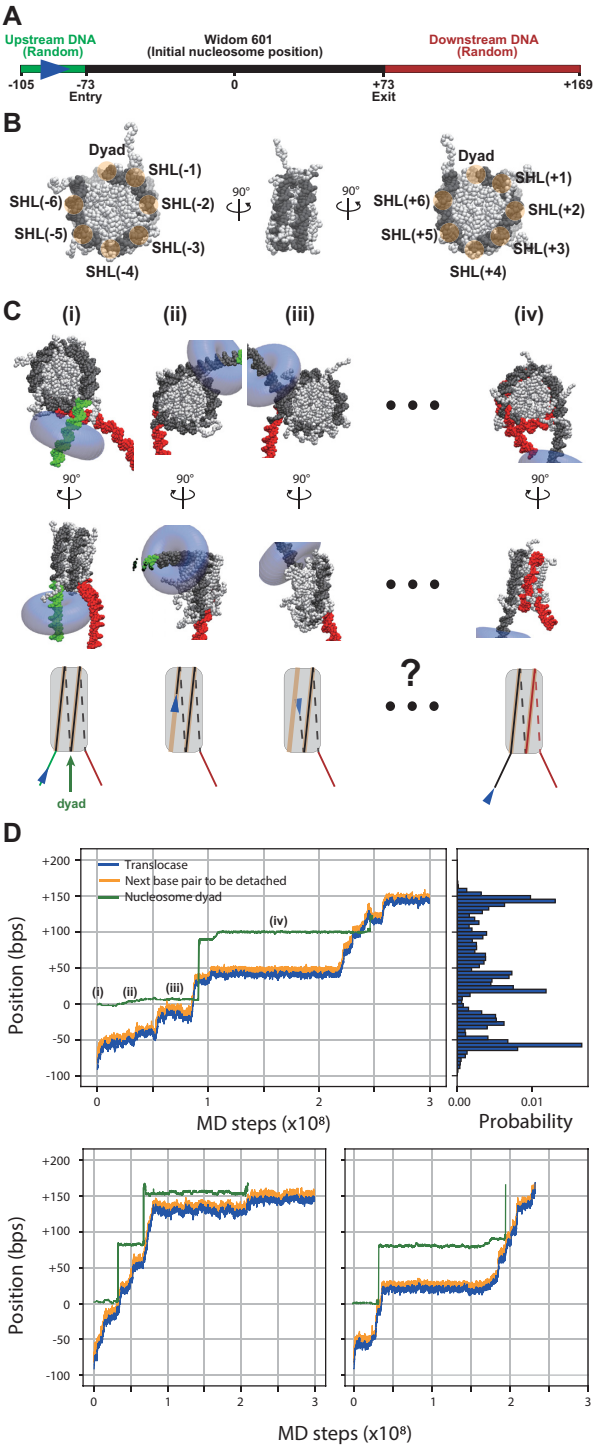

Figure 1. Molecular dynamics simulations of nucleosome being unwrapped by a translocase. (**A**) The map of the DNA sequence used in the simulations. In the initial structure, the Widom 601 nucleosome positioning sequence DNA wraps around a histone octamer to form a nucleosome. The base-pairs are numbered so that the dyad base-pair position in the initial structure becomes ± 0 bp. (**B**) Coarse-grained model of a nucleosome with the definitions of superhelical locations (SHL). (**C**) Snapshots from a simulation and their cartoon representations. The translocase and the histone octamer are colored blue and grey, respectively. The DNA is colored according to the color scheme in (A). (**D**) Representative simulation trajectories of the positions of the translocase, the base-pair to be detached, and the dyad (top left panel and bottom panels) and a probability distribution of the translocase position (top right panel).

parameters σ, ε, d_{M_r}, and d_{m_r} to 1.0 Å, 1.0 kcal/mol, 35 Å and 22.5 Å, respectively.

In the initial structure, the –92th (a relative position from the dyad) base-pair is at the center of the torus. Translocation was realized by applying a 14-pN force in the upstream direction (half of the stall force [28 pN] of the bacterial RNAP (28)) to the base-pair closest to the center of the torus (six DNA beads; 2.3 pN per each). This procedure models a processive motion of a translocase along DNA toward a nucleosome. DNA was not twisted in this pulling procedure.

We performed 80 pulling simulations and two sets of 80 non-pulling relaxation simulations in which either –54th or –14th base-pair was fixed at the center of the torus. All the simulations were performed using the software CafeMol 3.2 (https://www.cafemol.org) (29). The equations of motion were integrated over time by Langevin dynamics with the time step set to 0.3 cafemol time (∼14.7 fs). The monovalent ion concentration in the Debye-Hückel model was set to 300 mM, unless otherwise indicated, for the following reasons. First, the Debye-Hückel model cannot accurately treat specific features of divalent ions such as the high charge density and the preferential co-localization with the phosphate atoms on DNA. Second, the local monovalent ion concentration around DNA tends to get higher than what expected based on the Debye–Hückel approximation. To include these effects, we needed to set the monovalent ion concentration relatively high, as a first approximation.

Restriction enzyme digestion assay

To validate the molecular mechanism proposed based on the MD simulations, we performed restriction enzyme digestion assays. In the assays, we measured accessibility of the restriction enzymes, BssSI-v2 and EcoRI, to their restriction sites, one in the modified Widom 601 nucleosome-positioning sequence and the other in the downstream sequence to which a nucleosome is predicted to be repositioned upon the collision (Figure 3A and Supplementary Table S1). Before measuring, a T7 RNAP transcribed the DNA substrate from the T7 promoter site next to the positioning sequence and stalled at the –54th, –29th or –14th base-pair. The stall was realized in the absence adenosine triphosphate (ATP) in solution by exchanging adenine and thymine in some base-pairs in the positioning sequence so that the polymerase, for the first time, encounter thymine in the template strand at the stall site.

The T7_601_stall_-54, T7_601_stall_-29, and T7_601_stall_-14 DNA substrates (Supplementary Table S1) were chemically synthesized (Eurofins genomics; Supplementary Table S1) and amplified by polymerase chain reactions. We purified budding yeast histone proteins (H2A, H2B, H3 and H4) using an E. coli protein expression system and reconstituted nucleosomes using the purified proteins and the amplified DNA substrates as described previously (30). The reconstitution was confirmed by micrococcal nuclease (MNase) assays in which MNases (M0247S, New England BioLabs) digest linker DNA for 30 min and the digested products were run on 1% agarose gel. *In vitro* transcription on the DNA substrates was performed using HiScribe T7 High Yield RNA synthesis kit (E2040S, New England BioLabs) for 120 minutes (min) at 37 °C in the presence of 1 mM GTP, 1 mM CTP, and 1 mM UTP when otherwise specified. Next, we added 1 μL of RNase I (M0243, New England BioLabs) to reactions in 1 × NEBuffer 3.1 (B7003, New England BioLabs) and incubated for 30 min at 37°C to remove the transcripts. Then, we exchanged the buffer for the CutSmart buffer (B7204 New England BioLabs) using a 10K MWCO Amicon Ultra-0.5 Centrifugal Filter (UFC510024, Merck), added BssSI-v2 (R0680, New England BioLabs) or EcoRI-HF (R3101, New England BioLabs), and incubated for 15 min at 37°C. The digested products were extracted using phenol:chloroform:isoamyl (25:24:1) solution (Nakalai Tesque) and run on a 1% agarose gel. The gel was imaged using the iBright FL1500 imaging system (Thermo Fisher Scientific) and was analyzed using ImageJ software (31).

Deep sequencing assay

To investigate the nucleosome position after the collision, we performed deep sequencing assays. In these assays, a T7 RNAP transcribes on nucleosome reconstituted DNA and stalls at the –54th or –14th base-pair as described above. After the stall, the DNA substrates were digested by MNases, and the digested products were sequenced using the MinION R9.4.1 nanopore flowcell (Oxford Nanopore Technologies). The nucleosome reconstitution, transcription, and MNase digestion procedures were the same as described above. After the MNase digestion, we purified the digested products using a spin column (A9281, Promega) to avoid organic solvent contamination. We prepared a DNA library using the ligation kit (SQK-LSK109, Oxford Nanopore Technologies) and loaded the library into the flowcell according to the manufacturer's instruction. The signals from the device were analyzed using the MinKNOW software (Oxford Nanopore Technologies) to obtain sequence reads.

Calculation of free energy of nucleosome assembly

The free energy of nucleosome assembly along the DNA sequence was estimated using a Markov model described in Ref. (32), which is based on Monte-Carlo simulations of nucleosomes (33) at 300 K using a rigid-base pair model of DNA (34). To estimate the free energy of nucleosome assembly, we only take into account the DNA section up to the last contacts with the central H3/H4 tetramer (±28 bp away from the dyad), since both our tests and other studies found this to be a better predictor of nucleosome positioning along DNA (35).

RESULTS

Simulations of nucleosomal DNA unwrapping by a translocase

We performed coarse-grained MD simulations to investigate nucleosome repositioning when a translocase partially unwraps nucleosomal DNA. The simulation system contains the Widom 601 nucleosome-positioning DNA sequence flanked by random 32 and 96 bp DNA sequences upstream and downstream, respectively, together forming

275 bp DNA (Figure 1A, Supplementary Table S1. The base-pairs are numbered relative to the dyad of the 601 sequence). Initially, the nucleosome forms on the 601 sequence. A model DNA translocase initially loaded on the upstream DNA proceeds in the downstream direction, colliding with the nucleosome.

In these simulations, for histones, we used the coarse-grained model in which one particle represents one amino acid (36). A structure-based potential stabilizes the native structure of the histone octamer (27). The interactions between the histones were adjusted so that the complex disassembles in the absence of DNA (37). For DNA, we used the coarse-grained model in which three particles represent one nucleotide (24). Histone–DNA interactions include electrostatic interactions, excluded volume effects, and hydrogen bonds. These setups have been previously calibrated and already applied to investigate nucleosome dynamics (24). The nucleosome structure was modeled based on the crystal structures (PDB ID: 1KX5 (25) and 3LZ0 (26)) (Figure 1B). We modeled the translocase as a torus-shaped excluded volume potential. The translocation was realized by applying 14-pN force toward the upstream direction (half of the stall force [28 pN] of the bacterial RNA polymerase (28)) to the base-pair most proximal to the center of the torus. The force causes the next downstream base-pair to be pulled into the torus; when this base-pair becomes the closest to the torus center, the force is then applied to this new base-pair. The repetition of this procedure leads to a processive DNA translocation. Overall, the translocase relatively moves toward the nucleosome.

In the initial structure, the translocase was placed at 91 bp upstream from the dyad (Figure 1C (i), D top left panel, and Supplementary Figure S2). As the simulation proceeded, the translocase collided with the nucleosome, unwrapping the nucleosomal DNA. Note that the position of the translocase (the center of the torus) was, on average, 7 bp behind that of the base-pair to be detached (Figure 1D top left panel) due to the excluded volume of the translocase. When the translocase reached to –63 ± 2 bp and to –29 ± 5 bp, it stalled due to the relatively strong interaction between the base-pairs to be detached and the histone octamer (Figure 1C (ii), (iii), D top left panel, and Supplementary Figure S4). We calculated the probability distribution of the torus position from 80 simulation runs and found that the translocase statistically tended to stall at –57 ± 2 bp and –29 ± 5 bp before reaching the dyad (Figure 1C top right panel), consistent with the previous reports (38–40). In the current work, the translocase can partially unwrap the Widom 601 strong nucleosome positioning sequence wrapping around the histone octamer. Thus, it is reasonable to assume that the partial unwrapping can take place for the nucleosomes with a variety of DNA sequences.

Interestingly, after the translocase escaped from the –29 ± 5 bp stall, the DNA base-pairs located at the dyad (green line in Figure 1D, top left panel) made a sudden and large transition, accompanied by the translocase movement (Figure 1D, top left panel and Movie S1). We repeatedly observed the repositioning in the 80 simulations (Figure 1D, bottom panels and Supplementary Figure S2). In these simulations, the dyad repositioning distance ranged from 78 to 102 bp (Figure 1D, and Supplementary Figure S2). In the repositioned nucleosome, the entry-side half of the histone octamer was wrapped by the right half of the 601 sequence and the exit-side half by the random downstream DNA (Figure 1A, C (iv), and Supplementary Figure S4). After the nucleosome repositioning, the translocase stalls at 20 ± 2 bp (–63 ± 2 bp from the new dyad position; Figure 1D, top left panel), supporting the almost complete nucleosome formation. In some trajectories, we observed a second repositioning event, though the limited length of the downstream DNA precludes the complete nucleosome formation (Figure 1A and D, bottom left panel). In addition, we performed the simulations where the downstream random sequence was replaced with that of T7_601_stall_-54 (Supplementary Table S1) and obtained the similar results (Supplementary Figure S3), confirming that the nucleosome repositioning does not significantly depend on the downstream sequence.

Relaxation simulation of partially unwrapped nucleosome

This sudden and long-distance (78–102 bp) repositioning cannot be explained by the pushing model in which one base-pair unwrapping is coupled to one base-pair nucleosome repositioning. In our simulations, the force was applied as soon as the nucleotide enters the torus. In reality, however, the force must be generated at a certain stage of the ATP hydrolysis cycle (second time scale), which is much slower than our simulation microsecond timescale. Thus, the *in silico* translocation speed is much faster than reality in which the partially unwrapped nucleosome structure would relax every time the translocase moves one base-pair. To study this process, we performed a second set of simulations starting from a partially unwrapped nucleosome structure obtained in the above simulations. In this case, instead of pulling, we fixed the base-pair at the center of the torus at its initial position.

First, we performed 80 simulations using the nucleosome conformation in which the translocase was at the –18th base-pair as the initial structure (Figure 2A, top panel), which corresponds to just before the repositioning. As the simulation proceeds, the structure relaxed and significantly changed from the initial structure (Figure 2A and Movie S2). This result suggests that indeed the structure did not relax enough in the pulling simulations. In this new set of simulations, we observed the downstream repositioning in 61% (49/80) of the simulations.

Then, we sought to classify the structures in the 80 relaxation simulations. To achieve this, we calculated the contact maps of the histone octamer and DNA and performed a *k*-means clustering. The optimal numbers of clusters were decided to be seven based on the Calinski–Harabasz index (Supplementary Figure S5) (41), which is proportional to a ratio of inter- and intra-clusters dispersion. Visual inspection revealed that the seven clusters contain one initial state, one off-pathway intermediate state, two on-pathway intermediate states, and three final states. (Figure 2B and Supplementary Figure S6). The main pathway contains four of the seven states: one initial state, two on-pathway intermediate states, and one final state (Figure 2B, C and Supplementary Figure S6A). In the initial state, the –9th to 59th base-pairs contact with superhelical locations (SHL) (–1.5)

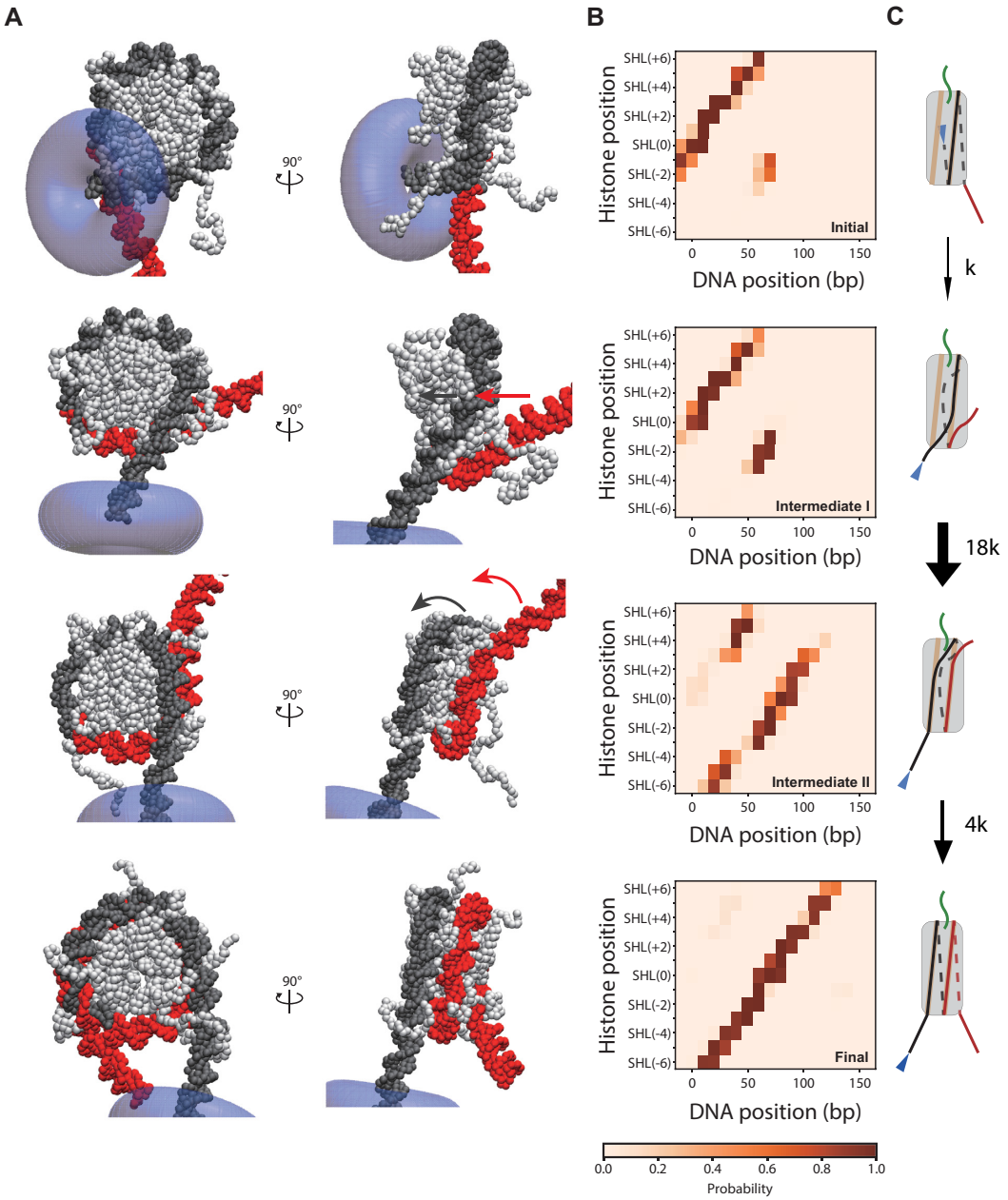

Figure 2. Relaxation simulations of the partially unwrapped nucleosome. (**A**) Representative structures in the simulation trajectories. DNA, the histones, and the translocase are colored according to the color scheme in Figure 1C. (**B**) Contact maps showing contacts between a histone octamer and DNA. The maps were averaged over the cluster members. See Figure 1B for the definition of SHL. (**C**) Cartoons explaining the lane-switch mechanism. The numbers next to the arrows represent relative transition rates.

to SHL (6.5) amino acids (Figure 2B, C, top panel; see Figure 1B for the positions of SHL). In the intermediate I state, the probability of contacts between the -9th to 3rd base-pairs and SHL (–1.5) to SHL (0.5) amino acids decreases, and that between the 59th to 71st base-pairs and the same amino acids increases (Figure 2B, C, second panel). This result indicates the competitive binding of the –9th to 3rd base-pairs and the 59th to 71st base-pairs to the same amino acids. In the intermediate II state, the probability of contacts between the 3rd to 34th base-pairs and SHL (0.5) to SHL (3.5) amino acids decreases, and that between the 19th to 40th base-pairs and SHL (–6.5) to SHL (–3.5) amino acids increases (Figure 2B, C, third panel). In this state, the DNA originally in the exit side switched its lane (the binding site on the histone octamer). In the final state, the 18th to 145th base-pairs bind to SHL (–6.5) to SHL (6.5) amino acids, fully wrapping around the histone octamer (Figure 2B, C, bottom panel). This state corresponds to the state after repositioning.

Based on the simulations, we computed the transition rates between the states along the repositioning pathway. Denoting the transition rate from the initial to intermediate I state as k ($= 8.1 \times 10^{-9}$ step^{-1}), the rates from the intermediate I to intermediate II state, and from the intermediate II

to final state are 19.7 ± 6.4 k and 4.0 ± 4.9 k, respectively (Figure 2C and Supplementary Figure S6). This result suggests that spontaneous DNA dissociation after partial unwrapping is the bottleneck transition of downstream repositioning.

Next, we used the nucleosome structure in which the translocase is at the –31st base-pair as an initial structure. In 93% (74/80) of these simulations, the histone octamer kept binding to the initial position (Supplementary Figure S7). In the remaining (6/80) simulations, H2A/H2B dimers dissociated from the H3/H4 tetramer. Interestingly, we did not observe downstream repositioning in these simulations (0/80). This is in sharp contrast to the simulations started at the –18th base-pair, where we observed downstream repositioning in 61% (49/80) of the runs. Note that, when the translocase is at the –31st base-pair and at the –18th base-pairs, the next base-pairs to be detached are at the –19th base-pairs and at the -9th base-pairs, respectively. Thus, the simulation results suggest that the detachment of the –19th to –9th base-pairs from the histone octamer is essential for downstream repositioning.

Based on these simulations, we propose the lane-switch mechanism. In this mechanism, after a translocase unwraps nucleosomal DNA up to the site proximal to the dyad, the remaining wrapped DNA switches its binding region (lane) to that just vacated by the unwrapping, and then the downstream DNA rewraps, completing downstream repositioning. In the simulations, the several base-pairs of the wrapped end DNA occasionally dissociate from and re-associate to the histone octamer. Such breathing dynamics have also been observed experimentally, though the end position was altered by the translocase. This temporary and spontaneous dissociation allows H3 and H2B tails to pass under DNA. These tails are disordered polypeptides that occasionally become compact. These conformational changes may also help the tails to pass under DNA. Collectively, the breathing dynamics, together with the conformational flexibility of the tails, may be necessary to facilitate the lane switching. Next, we sought to validate the lane-switch mechanism experimentally.

Restriction enzyme digestion assay

To validate the model, we chose the T7 RNAP as a model system. First, we designed 498 bp DNA substrates containing the T7 promoter and the nucleosome positioning sequence (Figure 3A and Supplementary Table S1). As the positioning sequence, the Widom 601 sequence was modified so that the template strand does not contain thymine from the entry nucleotide to one nucleotide before the stall site. The stall sites were chosen at the –54th, –29th and –14th base-pairs (relative position from the center of the positioning sequence) (Figure 3A and Supplementary Table S1). MNase-seq assay (42) confirmed that this modification does not significantly affect nucleosome positioning (Supplementary Figure S8). When these DNA substrates were transcribed by the T7 RNAP in the absence of ATP in solution, transcription was terminated at these stall sites (Supplementary Figure S9A).

The designed sequences contain the BssSI restriction site in the modified 601 sequence, which is supposed to be occluded by a histone octamer (43). The sequences also contain the EcoRI restriction site, which is supposed to be occluded when the histone octamer repositions downstream upon transcription. Thus, the repositioning frequency can be quantified by the restriction enzyme digestion assay (Figure 3B). In this assay, we digested the DNA substrates with BssSI and EcoRI and run the products on 1% agarose gel (Supplementary Figure S10). The digested and undigested fragments were separated on a gel, and the intensities of the undigested product were measured (Figure 3C). We defined the $\Delta_{occlusion}$ as the intensity after transcription divided by the intensity before transcription.

For the naked DNA, the values of $\Delta_{occlusion}$ were about one irrespective of the enzymes and the stall sites (Figure 3D and Supplementary Figure S10), suggesting that the enzymes can bind to the restriction sites when the T7 RNAP stalls at the –54th, –29th or –14th base-pair. When a nucleosome was reconstituted on the DNA substrates, $\Delta_{occlusion}$ of EcoRI after transcription was 2.1 ± 0.2, 3.7 ± 1.4, and 11.6 ± 3.5 for stalling at the –54th, –29th and –14th base-pairs, respectively (Figure 3D). The MNase assay confirmed nucleosome formations before and after transcription (Supplementary Figure S9B). These results suggests that the nucleosome repositions downstream when the T7 RNAP proceeds to the –14th base-pair. On the other hand, $\Delta_{occlusion}$ of BssSI was 0.8 ± 0.1, 0.6 ± 0.2, and 0.4 ± 0.2 for stalling at the –54th, –29th and –14th base-pairs, respectively (Figure 3D). Thus, the BssSI site in the nucleosome positioning sequence was more exposed when T7 RNAP proceeds to the –14th base-pair, as expected from an increased probability of downstream repositioning.

To check if a nucleosome repositions by temporary dissociation and re-association of a histone octamer, we performed the same assay using naked DNA in the presence of histone octamers in solution. As a result, $\Delta_{occlusion}$ was about one irrespective of the enzymes and the stall sites (Figure 3D), suggesting that, once in solution, the histone octamers do not occlude the BssSI or EcoRI site. This result argues against the temporary dissociation and re-association of the histone octamer as the mechanism for downstream repositioning.

Together, the enzyme digestion assays support our model of nucleosome downstream repositioning coupled with DNA unwrapping.

Deep sequencing assay

In the restriction enzyme digestion assay, we could not identify the nucleosome position down to base-pair resolution. To localize the complex, the substrates before and after the transcription was digested by MNases, and the digested products were sequenced using a nanopore sequencer (44). MNases do not efficiently digest the DNA wrapping around a histone octamer. Thus, we can use the sequence reads from the nanopore sequencer as a proxy for a nucleosome position.

First, a nucleosome was reconstituted using the DNA substrate described above (Figure 3A). Then, the substrate was digested, purified, and sequenced. The distribution of the read length shows a single peak around 158 bp (Supplementary Figure S11). This result indicates that the se-

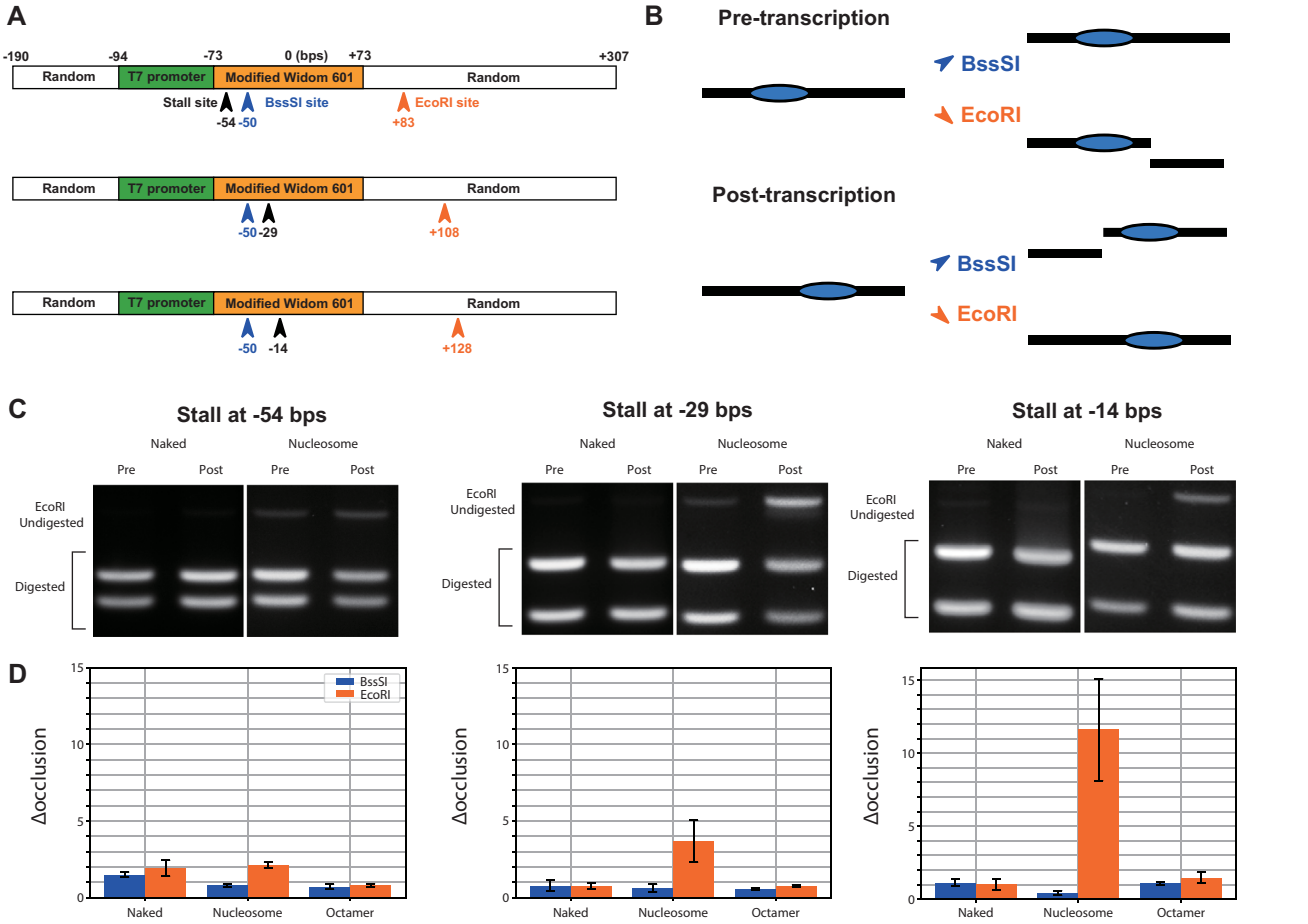

Figure 3. Restriction enzyme digestion assay. (**A**) The DNA sequence map of substrates used in the assay. The T7 RNAP stall sites where the translocase first encounter thymine are marked by the black arrows. BssSI and EcoRI restriction sites are marked by the blue and orange arrows, respectively. (**B**) Cartoons of the experimental setup. At the pre-transcription stage, the BssSI site, but not the EcoRI site, is occluded by the histone octamer. On the other hand, if the nucleosome repositions upon transcription according to the lane-switch mechanism, the EcoRI site, but not the BssSI site, is occluded by the histone octamer. (**C**) Images of 1% agarose gel on which the EcoRI-digested products run. The DNA substrates were digested at the pre- and post-transcription stages. (**D**) Plot showing the intensity of the undigested band at pre-transcription stage divided by that of the post-transcription stage ($\Delta_{occlusion}$). The assay was repeated using naked DNA (Naked), nucleosome reconstituted DNA (nucleosome), and the naked DNA with histone octamers in solution (octamer).

quenced products wrap around histone octamers before the purification. We define the position of the central base-pair of the read as a nucleosome position. Only sequence reads with length from 146 to 170 bp are considered for the analysis.

Next, after the nucleosome reconstitution, the T7 RNAP transcriptions were induced in the absence of ATP in solution. The DNA substrates contain the stall site at the –14th or –54th base-pair as described above. After transcription, the substrates were digested, purified, and sequenced.

In the case of the stall position at the –54th base-pair, the frequency distribution of the nucleosome position shows a peak around 50 bp (Figure 4A). This peak bears two interpretations: (i) unwrapping of each base-pair is coupled with one base-pair nucleosome repositioning (pushing), or (ii) the nucleosome spontaneously slides to this meta-stable positioning site due to the occlusion of the modified 601 sequence by the T7 RNAP (spontaneous sliding). However, when the T7 RNAP proceeds up to the –54th base-pair, the pushing model would predict repositioning by up to 19 bp, which is inconsistent with the 50 bp peak (Figure 4E).

Interestingly, in the case of the stall position at the –14th base-pair, the frequency distribution of the reposition distance shows two peaks (Figure 4B) around 50 and 100 bp. When the T7 RNAP proceeds to the –14th base-pair, the pushing model predicts repositioning by 59 bp, which is inconsistent with the 100 bp peak. On the other hand, the 100 bp peak (101 ± 8-bp in Figure 4B) is within the 78–102 bp range of the repositioning distance predicted by the lane-switch mechanism (Figure 4E). Thus, we concluded that the 100 bp peak in the frequency distribution of reposition distance supports the lane-switch mechanism. The following two pieces of circumstantial evidence support that the 100 bp peak is not caused by the spontaneous nucleosome sliding. First, the peak appears in 10 min, though the time scale of the spontaneous nucleosome sliding is usually assumed to be hours. Second, the theoretically predicted free energy landscape of the nucleosome positioning suggests that the

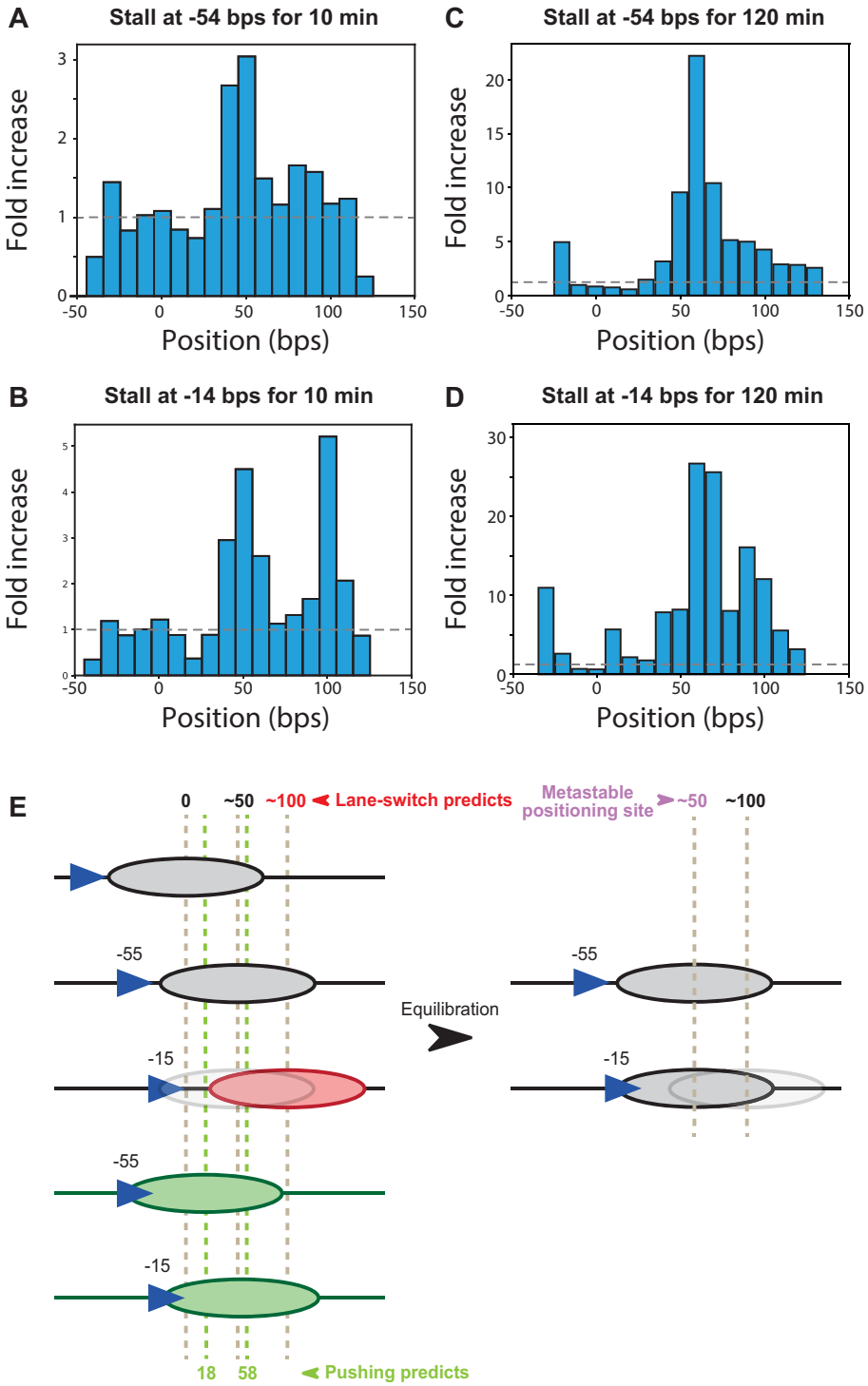

Figure 4. MNase-seq assay. (A–D) Frequency distribution of a nucleosome position at the post-transcription stage. The origin corresponds to the position of the center base-pair of the Widom 601 nucleosome positioning sequence. The distribution was normalized by dividing by the distribution at the pre-transcription stage. The RNAP stalls at the –54th base-pair for 10 min (**A**), at the –14th base-pair for 10 min (**B**), at the –54th base-pair for 120 min (**C**), and at the –14th base-pair for 120 min (**D**). (**E**) Cartoons of interpretation of the experimental data.

sequence around +100 bp does not form stable nucleosome (Supplementary Figure S12).

Next, we consider the mechanism behind the 50 bp peak, which was observed irrespective of the stall position. This peak is best explained by the spontaneous sliding model because of the following reasons: (i) If the unwrapping of each base-pair were coupled with the one base-pair reposition of the histone octamer, the frequency distribution should show peaks around 19 and 59 bp in the case of stalling at the –54th and –14th base-pairs, respectively, which were not observed. (ii) The theoretically predicted free energy landscape of the nucleosome positioning shows a meta-stable basin around 50 bp (Supplementary Figure S12), indicating that the site can become the preferred destination site for the spontaneous sliding once the T7 RNAP destabilizes the positioning at 0 bp. (iii) When T7 RNAP stalling at the –15th base-pair is prolonged (for 120 min instead of 10 min), giving the nucleosome more time to slide toward its equilibrium position, the relative heights of the two peaks changes, increasing for the 50 bp peak and decreasing for the 100 bp peak (Figure 4B and D). Also, when T7 RNAP stalls at the –54th base-pair for 120 min, the 50 bp peak gets sharper (Figure 4A and C), supporting that this is one of the stable destination sites for the spontaneous sliding. If the stalled T7 RNAP had dissociated from DNA, we could have observed decrease of the +50 bp peak since nucleosome should tend to slide toward the Widom 601 sequence, which is not the case. Thus, we assume that the T7 RNAP stayed binding to DNA for 120 min. These considerations make us conclude that the 50 bp peak can be explained by the spontaneous sliding model. Despite the existence of such metastable sites, T7 RNAP repositions the nucleosome to the distal 100 bp sites when it unwraps to the –15th but not –55th base-pair (Figure 4E), supporting the lane-switch mechanism.

Together, the MD simulations, the enzyme digestion assays, and the MNase-seq assays consistently suggest that the nucleosome repositions downstream through the lane-switch mechanism.

DISCUSSION

In this study, we sought to elucidate the molecular mechanism by which a nucleosome repositions when a translocase unwraps nucleosomal DNA. To achieve this, we performed MD simulations, restriction enzyme digestion assays, and deep sequencing assays. Our MD simulations in which a model translocase unwraps nucleosomal DNA (Figure 1) revealed that the nucleosome repositions downstream upon unwrapping. Further structural relaxation simulations (Figure 2) revealed the detailed molecular mechanism of downstream repositioning. In this mechanism, after a translocase unwraps nucleosomal DNA up to the site proximal to the dyad, the remaining wrapped DNA switches its binding region (lane) to that vacated by the unwrapping, and finally the downstream DNA rewraps, completing downstream repositioning. The enzyme digestion assays (Figure 3) and the deep sequencing assay (Figure 4) experimentally supported the mechanism.

Previous studies proposed the Pol II-type (9–16) and Pol III-type (9,17–21) molecular mechanisms of nucleosome repositioning upon nucleosome unwrapping. In the Pol II-type mechanism, the translocase passes through the nucleosome without changing the position of the nucleosome. To realize this, the histone octamer electrostatically interacts with the translocase, forming the Ø-intermediate structure. On the other hand, in the Pol III-type mechanism, a nucleosome repositions upstream. Notably, the Pol III-type mechanism was proposed based on experiments in which the nucleosome was reconstituted at the downstream end of DNA, precluding downstream repositioning (9,17–21). In the current work, we removed this constraint by reconstituting nucleosome at the middle of the DNA substrate, showing that a nucleosome repositions downstream upon nucleosome partial unwrapping. Whether a nucleosome repositions downstream or upstream may depend on the availability of DNA, which is regulated by its persistence length and occlusion by other proteins. The ionic strength dependence of the repositioning mechanism and, ultimately, the relevant mechanism in cellular environment should be addressed in future.

Gottesfeld and Luger reported that T7 RNAP stalls at the entry base-pair when the pyrrole-imidazole polyamides binding to the dyad, preventing the nucleosome repositioning (22). This result supports the mechanism by which one base-pair unwrapping is coupled to one base-pair repositioning (the pushing model). However, the study did not fully exclude the possibility that the polyamide spatially proximal to the entry site directly affects the T7 RNAP translocation. In fact, it was reported that T7 RNAP can partially unwrap nucleosomal DNA without nucleosome repositioning (9,17–20). Also, the current study shows that repositioning does not take place until a translocase partially unwraps nucleosomal DNA. Though the current study does not fully exclude the possibility that the repositioning based on the pushing mechanism take place, in our deep sequencing assay, we clearly observed repositioning which cannot be explained by the pushing mechanism but can be explained by the lane-switch mechanism.

In the current study, we propose that the nucleosome repositions according to the lane-switch mechanism when there is little attractive interaction between a translocase and a histone octamer. This indicates that other types of repositioning mechanisms should be based on an intricate interaction network between the translocase and the histone octamer. For example, Pol II can bypass a nucleosome without histone octamer repositioning because of strong electrostatic interaction between the translocase and the complex (15). The lane-switch mechanism represents a fundamental passive mechanism useful for understanding the molecular basis of transcription through nucleosome, histone recycling, and nucleosome remodeling, where more intricate interaction between translocase and the histone octamer must be involved in.

DATA AVAILABILITY

The data that support the findings of this study are available from the corresponding author upon reasonable request.

SUPPLEMENTARY DATA

Supplementary Data are available at NAR Online.

ACKNOWLEDGEMENTS

We thank members of the theoretical biophysics laboratory at Kyoto University for discussions and assistance throughout this work. Also, we thank Prof. Hitoshi Kurumizaka and his laboratory members for helping us to purify histones and reconstituting nucleosome.

FUNDING

PRESTO [JPMJPR19K3 to T.T.]; Grant-in-Aid for Scientific Research B [19H03194 to T.T.]; Grant-in-Aid for Scientific Research on Innovative Areas (Molecular Engine) [19H05392 to T.T.]; Grant-in-Aid for Scientific Research on Innovative Areas (Chromatin Potential) [19H05260 to T.T.]; CREST grant of Japan Science and Technology Agency (JST) [JPMJCR1762 to S.T.]. Funding for open access charge: CREST grant of Japan Science and Technology Agency (JST) [JPMJCR1762 to S.T.].
Conflict of interest statement. None declared.

REFERENCES

1. Luger,K., Armin,M.W., Robin,R.K., David,S.F. and Timothy,R.J. (1997) Crystal structure of the nucleosome core particle at 2.8 Å resolution. *Nature*, **389**, 251–260.
2. Finkelstein,I.J. and Greene,E.C. (2013) Molecular traffic jams on DNA. *Annu. Rev. Biophys.*, **42**, 241–263.
3. Singleton,M.R., Dillingham,M.S. and Wigley,D.B. (2007) Structure and mechanism of helicases and nucleic acid translocases. *Annu. Rev. Biochem.*, **76**, 23–50.
4. Routh,A., Sandin,S. and Rhodes,D. (2008) Nucleosome repeat length and linker histone stoichiometry determine chromatin fiber structure. *Proc. Natl Acad. Sci. U.S.A.*, **105**, 8872–8877.
5. Tennyson,C.N., Klamut,H.J. and Worton,R.G. (1995) The human dystrophin gene requires 16 hours to be transcribed and is cotranscriptionally spliced. *Nat. Genet.*, **9**, 184–190.
6. Finkelstein,I.J., Visnapuu,M.-L. and Greene,E.C. (2010) Single-molecule imaging reveals mechanisms of protein disruption by a DNA translocase. *Nature*, **468**, 983–987.
7. Terakawa,T., Redding,S., Silverstein,T.D. and Greene,E.C. (2017) Sequential eviction of crowded nucleoprotein complexes by the exonuclease RecBCD molecular motor. *Proc. Natl Acad. Sci. U.S.A.*, **114**, E6322–E6331.
8. Lai,W.K.M. and Pugh,B.F. (2017) Understanding nucleosome dynamics and their links to gene expression and DNA replication. *Nat. Rev. Mol. Cell Biol.*, **18**, 548–562.
9. Bednar,J., Studitsky,V.M., Grigoryev,S.A., Felsenfeld,G. and Woodcock,C.L. (1999) The nature of the nucleosomal barrier to Transcription: Direct observation of paused intermediates by electron cryomicroscopy. *Mol. Cell*, **4**, 377–386.
10. Kireeva,M.L., Walter,W., Tchernajenko,V., Bondarenko,V., Kashlev,M. and Studitsky,V.M. (2002) Nucleosome remodeling induced by RNA polymerase II. *Mol. Cell*, **9**, 541–552.
11. Walter,W., Kireeva,M.L., Studitsky,V.M. and Kashlev,M. (2003) Bacterial polymerase and yeast polymerase II use similar mechanisms for transcription through nucleosomes. *J. Biol. Chem.*, **278**, 36148–36156.
12. Hodges,C., Bintu,L., Lubkowska,L., Kashlev,M. and Bustamante,C. (2009) Nucleosomal fluctuations govern the transcription dynamics of RNA polymerase II. *Science*, **325**, 626–628.
13. Kulaeva,O.I., Gaykalova,D.A., Pestov,N.A., Golovastov,V.V., Vassylyev,D.G., Artsimovitch,I. and Studitsky,V.M. (2009) Mechanism of chromatin remodeling and recovery during passage of RNA polymerase II. *Nat. Struct. Mol. Biol.*, **16**, 1272–1278.
14. Bintu,L., Kopaczynska,M., Hodges,C., Lubkowska,L., Kashlev,M. and Bustamante,C. (2011) The elongation rate of RNA polymerase determines the fate of transcribed nucleosomes. *Nat. Struct. Mol. Biol.*, **18**, 1394–1399.
15. Chang,H.-W., Kulaeva,O.I., Shaytan,A.K., Kibanov,M., Kuznedelov,K., Severinov,K.V., Kirpichnikov,M.P., Clark,D.J. and Studitsky,V.M. (2014) Analysis of the mechanism of nucleosome survival during transcription. *Nucleic Acids Res.*, **42**, 1619–1627.
16. Gaykalova,D.A., Kulaeva,O.I., Volokh,O., Shaytan,A.K., Hsieh,F.-K., Kirpichnikov,M.P., Sokolova,O.S. and Studitsky,V.M. (2015) Structural analysis of nucleosomal barrier to transcription. *Proc. Natl Acad. Sci. U.S.A.*, **112**, E5787–E5795.
17. Clark,D.J. and Felsenfeld,G. (1992) A nucleosome core is transferred out of the path of a transcribing polymerase. *Cell*, **71**, 11–22.
18. Studitsky,V.M., Clark,D.J. and Felsenfeld,G. (1994) A histone octamer can step around a transcribing polymerase without leaving the template. *Cell*, **76**, 371–382.
19. Studitsky,V.M., Clark,D.J. and Felsenfeld,G. (1995) Overcoming a nucleosomal barrier to transcription. *Cell*, **83**, 19–27.
20. Walter,W. and Studitsky,V.M. (2001) Facilitated transcription through the nucleosome at high ionic strength occurs via a histone octamer transfer mechanism. *J. Biol. Chem.*, **276**, 29104–29110.
21. Studitsky,V.M. (1997) Mechanism of transcription through the nucleosome by Eukaryotic RNA polymerase. *Science*, **278**, 1960–1963.
22. Gottesfeld,J.M., Belitsky,J.M., Melander,C., Dervan,P.B. and Luger,K. (2002) Blocking transcription through a nucleosome with synthetic DNA ligands. *J. Mol. Biol.*, **321**, 249–263.
23. Li,W., Wang,W. and Takada,S. (2014) Energy landscape views for interplays among folding, binding, and allostery of calmodulin domains. *Proc. Natl Acad. Sci. U.S.A.*, **111**, 10550–10555.
24. Freeman,G.S., Hinckley,D.M., Lequieu,J.P., Whitmer,J.K. and de Pablo,J.J. (2014) Coarse-grained modeling of DNA curvature. *J. Chem. Phys.*, **141**, 165103.
25. Davey,C.A., Sargent,D.F., Luger,K., Maeder,A.W. and Richmond,T.J. (2002) Solvent mediated interactions in the structure of the nucleosome core particle at 1.9Å resolution. *J. Mol. Biol.*, **319**, 1097–1113.
26. Vasudevan,D., Chua,E.Y.D. and Davey,C.A. (2010) Crystal structures of nucleosome core particles containing the '601' Strong positioning sequence. *J. Mol. Biol.*, **403**, 1–10.
27. Niina,T., Brandani,G.B., Tan,C. and Takada,S. (2017) Sequence-dependent nucleosome sliding in rotation-coupled and uncoupled modes revealed by molecular simulations. *PLoS Comput. Biol.*, **13**, e1005880.
28. Wang,M.D. (1998) Force and velocity measured for single molecules of RNA polymerase. *Science*, **282**, 902–907.
29. Kenzaki,H., Koga,N., Hori,N., Kanada,R., Li,W., Okazaki,K., Yao,X.-Q. and Takada,S. (2011) CafeMol: a coarse-grained biomolecular simulator for simulating proteins at work. *J. Chem. Theory Comput.*, **7**, 1979–1989.
30. Mashanov,G.I. and Batters,C. (eds). (2011) In: *Single Molecule Enzymology*. Methods and Protocols Humana Press, Totowa, NJ.
31. Abramoff,M.D., Magalhaes,P.J. and Ram,S.J. (2004) Image processing with ImageJ. *Biophotonics*, **7**, 36–42.
32. Tompitak,M., Barkema,G.T. and Schiessel,H. (2017) Benchmarking and refining probability-based models for nucleosome-DNA interaction. *BMC Bioinformatics*, **18**, 157.
33. Eslami-Mossallam,B., Schram,R.D., Tompitak,M., van Noort,J. and Schiessel,H. (2016) Multiplexing genetic and nucleosome positioning Codes: A computational approach. *PLoS One*, **11**, e0156905.
34. Olson,W.K., Gorin,A.A., Lu,X.-J., Hock,L.M. and Zhurkin,V.B. (1998) DNA sequence-dependent deformability deduced from protein-DNA crystal complexes. *Proc. Natl Acad. Sci. U.S.A.*, **95**, 11163–11168.
35. van der Heijden,T., van Vugt,J.J.F.A., Logie,C. and van Noort,J. (2012) Sequence-based prediction of single nucleosome positioning and genome-wide nucleosome occupancy. *Proc. Natl Acad. Sci. U.S.A.*, **109**, E2514–E2522.
36. Takada,S., Kanada,R., Tan,C., Terakawa,T., Li,W. and Kenzaki,H. (2015) Modeling structural dynamics of biomolecular complexes by coarse-grained molecular simulations. *Acc. Chem. Res.*, **48**, 3026–3035.
37. Brandani,G.B., Tan,C. and Takada,S. (2021) The kinetic landscape of nucleosome assembly: a coarse-grained molecular dynamics study. *PLoS Comput. Biol.*, **17**, e1009253.
38. Hall,M.A., Shundrovsky,A., Bai,L., Fulbright,R.M., Lis,J.T. and Wang,M.D. (2009) High-resolution dynamic mapping of

histone-DNA interactions in a nucleosome. *Nat. Struct. Mol. Biol.*, **16**, 124–129.
39. Chang,H.-W., Pandey,M., Kulaeva,O.I., Patel,S.S. and Studitsky,V.M. (2016) Overcoming a nucleosomal barrier to replication. *Sci. Adv.*, **2**, e1601865.
40. Boyer,J.A., Spangler,C.J., Strauss,J.D., Cesmat,A.P., Liu,P., McGinty,R.K. and Zhang,Q. (2020) Structural basis of nucleosome-dependent cGAS inhibition. *Science*, **370**, 450–454.
41. Calinski,T. and Harabasz,J. (1974) A dendrite method for cluster analysis. *Commun. Stats. Theory Methods*, **3**, 1–27.
42. Schones,D.E., Cui,K., Cuddapah,S., Roh,T.-Y., Barski,A., Wang,Z., Wei,G. and Zhao,K. (2008) Dynamic regulation of nucleosome positioning in the human genome. *Cell*, **132**, 887–898.
43. Polach,K.J. and Widom,J. (1995) Mechanism of protein access to specific DNA sequences in chromatin: a dynamic equilibrium model for gene regulation. *J. Mol. Biol.*, **254**, 130–149.
44. Jain,M., Koren,S., Miga,K.H., Quick,J., Rand,A.C., Sasani,T.A., Tyson,J.R., Beggs,A.D., Dilthey,A.T., Fiddes,I.T. *et al.* (2018) Nanopore sequencing and assembly of a human genome with ultra-long reads. *Nat. Biotechnol.*, **36**, 338–345.